Available online at www.sciencedirect.com

SCIENCE DIRECT®

Catalysis Today 112 (2006) 121–125

CATALYSIS TODAY

www.elsevier.com/locate/cattod

Influence of the active phase structure Bi-Mo-Ti-O in the selective oxidation of propene

S.R.G. Carrazán, C. Martín, R. Mateos, V. Rives *

Departamento de Química Inorgánica, Universidad de Salamanca, 37008-Salamanca, Spain

Abstract

Bismuth molybdenum titanium oxides were prepared in a highly dispersed state by the sol–gel method and in a largely crystallized state by coprecipitation and impregnation. The catalysts contained 14 or 25 wt.% of bismuth molybdate. Their catalytic performance in propene oxidation to acrolein was studied. The increase in activity of Bi-Mo-Ti oxides in propene oxidation as compared to that of bulk bismuth molybdate can be tentatively related, in the case of the sol–gel samples, to the stabilization of small aggregates of Bi- and Mo-containing phases due to the beneficial presence of the titania matrix. The catalytic performance of the samples prepared by coprecipitation or impregnation is enhanced once a crystal size of bismuth molybdate close to 23 nm is reached, i.e., the crystal size should not be too small (samples prepared by the sol–gel method) nor too large (samples prepared by impregnation and coprecipitation), but an optimum size should exist to enhance the catalytic performance.

Keywords: Bismuth molybdate; Crystal size; Catalytic oxidation; Propene; Acrolein

1. Introduction

Different commercial multicomponent catalysts have been developed to improve the efficiency of bismuth molybdate catalysts for acrolein and acrylonitrile synthesis via Mars and van Krevelen redox mechanism [1]. The active phase is bismuth molybdate in the α ($Bi_2Mo_3O_{12}$), β ($Bi_2Mo_2O_9$) or γ (Bi_2MoO_6) forms [2,3]. Most of these studies attempt to relate the physicochemical properties of these solids with their catalytic activity [4,5]. However, it is not clear enough which of the phases (α, β or γ) is more active and selective in allylic oxidation. On the other hand, several groups [6,7] have tested the effect of several supports (e.g., silica, alumina and titania) on the precise phase of bismuth molybdate formed and the interaction/collaboration between that phase and the support, aiming to find beneficial effects for the catalytic performance.

In this paper we report the synthesis of a series of Bi-Mo-Ti oxides following different routes (sol–gel, coprecipitation and impregnation) in order to analyse how the preparation method (and changes in several preparation parameters, such as bismuth molybdate loading, time and the calcination temperature) and the presence of the titania matrix modify the structure of the active phase in the partial oxidation of propene to acrolein. Moreover, we also try to relate the catalytic performance with the solid-state properties of the catalysts, especially from the structural point of view.

2. Experimental

2.1. Preparation of the catalysts

Catalysts Bi-Mo-Ti-O were prepared following three routes, namely coprecipitation (sample C1), impregnation (samples I1 and I2) and sol–gel (sample SG2). To prepare sample C1, a solution containing 0.35 g $Bi(NO_3)_3 \cdot 5H_2O$ (hereafter BiN) in 4 M HNO_3 was added to a suspension of 2 g of TiO_2 (Degussa P-25, ca. 80% anatase, 50 $m^2\,g^{-1}$) in a solution containing 0.1949 g $(NH_4)_6Mo_7O_{12} \cdot 4H_2O$ (hereafter AHM) in a 5 wt.% ammonia solution; the concentration of the BiN solution was that necessary to obtain a molar Mo/Bi ratio of 3/2 and final pH was adjusted to 7 with the same ammonia solution above described; in this way, precipitation of bismuth molybdate is achieved. The mixture was vigorously stirred and gently heated in a water bath to dryness. The solid thus obtained was dried in an open oven at 100 °C for 19 h, and finally calcined in an open

---

* Corresponding author. Fax: +349 23 29 45 74.
E-mail address: vrives@usal.es (V. Rives).

0920-5861/$ – see front matter © 2005 Elsevier B.V. All rights reserved.
doi:10.1016/j.cattod.2005.11.044

oven at 500 °C for 3 h. Samples I were obtained by adding first a AHM aqueous solution (containing 0.1954 or 0.3908 g) to 2 g of TiO_2; after evaporation of the solvent the solid was calcined in an open oven at 500 °C for 3 h and then it was suspended in a BiN/HNO_3 solution (containing 0.35 or 0.71 g BiN); drying and calcination were performed as above described. In this case two different samples were obtained: sample I1 containing 14 wt.% of bismuth molybdate (hereafter BM) and sample I2 containing 25% BM. Finally, to prepare sample SG2 by the sol–gel method, 7.34 g of Ti tetraisopropoxide were dissolved in 27.5 ml of isopropanol and, while vigorously stirred (500 rpm), solutions of AHM, BiN and HNO_3 (4 M) were simultaneously added. The molar water:alkoxide:acid ratio was 6:1:0.5 and the molar Mo/Bi ratio was 3/2, the total BM content was equivalent to 25%. Gelation took place in 2–3 min at room temperature and the gel was aged for 20 h. After that it was dried under vacuum at room temperature. The solid obtained was calcined in O_2 flow at 250 °C for 30 min to remove organic residues and then at 500 °C for further 30 min (in all cases, the heating schedule was 5 °C min^{-1}). The solid was cooled to room temperature under the oxygen flow.

In order to analyse the effect of the calcination time, portions of catalysts I2 and SG2 were calcined for 8 or 20 h, respectively, at 500 °C, leading to samples I2c and SG2c, respectively. Bulk α-$Bi_2Mo_3O_{12}$ (sample α-BM) was prepared by precipitation from aqueous AHM and BiN/HNO_3 solutions, as described elsewhere [8]: a portion of 10 g of BiN was dissolved in 42 ml of aqueous HNO_3 (4 M) to avoid bismuth hydrolysis. This solution was dropwise added on a 5% NH_3 aqueous solution of AHM containing the stoichiometric amount of AHM) and pH was also adjusted to 7, thus precipitating bismuth molybdate. Finally, the precipitate was dried and the solid was calcined in flowing oxygen at 5 °C min^{-1} up to 250 °C; this temperature was maintained for 30 min and then was raised up to 500 °C at the same heating rate, and this temperature was also maintained for 30 min. Then the sample was cooled to room temperature under oxygen flow.

2.2. Experimental techniques

Element chemical analyses were carried out by atomic absorption in a Mark-2 ELL 240 apparatus at Servicio General de Análisis Químico Aplicado (University of Salamanca, Spain). The powder X-ray diffraction (PXRD) patterns were obtained with a Siemens D-500 diffractometer using Cu Kα radiation (λ = 1.5418 Å) interfaced to a DACO-MP data acquisition microprocessor, the identification of the phases was achieved by using a database software (JCPDS files). The average crystallite sizes were estimated using the Scherrer equation and the width of selected diffraction peaks were fitted by a Pearson-type profile function. An instrumental line broadening of $2\theta = 0.23^\circ$ was taken into account. The FT-Raman spectra were recorded in a RFS 100/S Bruker spectrophotometer using the 1064 nm line from a Nd:YAG laser as the excitation line, with an output laser power of 150 mW; the resolution was 4 cm^{-1} and a backscattering geometry was chosen. Specific surface area, following the BET method, and porosity assessment were determined from nitrogen adsorption–desorption isotherms, recorded at −196 °C in a Gemini apparatus from Micromeritics.

2.3. Catalytic tests

Selective oxidation of propene was studied under atmospheric pressure conditions in a conventional fixed-bed reactor equipped with a jacket furnace. A PID controller with a coaxial thermocouple was used to control the temperature, and the reactions were carried out at 400 and 420 °C; the reaction mixture consisted of He:O_2:propene (molar ratio 10:10:80, corresponding to partial pressures of 76, 76 and 608 Torr, respectively), the flow (total 30 ml min^{-1}) being measured with mass flow controllers. Fifty milligrams of catalyst was dispersed with glass balls (diameter 200–315 μm). Analysis of the products was made on-line with an Intersmat IGC 121 ML gas chromatograph with a thermal conductivity detector and Hayesep Q (1.5 m length, 1/8 in. diameter) and Tenax (2.5 m length, 1/8 in. diameter) columns. Acrolein, CO_2 and water were the only reaction products.

3. Results and discussion

3.1. Characterisation

As the solids were not filtered after synthesis, the chemical analysis data indicate that the Bi, Mo and Ti content, and the molar Mo/Bi ratio (3/2) are coincident with the expected values.

The PXRD pattern of bulk bismuth molybdate (sample α-BM, Fig. 1) corresponds to monoclinic α-$Bi_2Mo_3O_{12}$, which most intense peaks are recorded at 3.19 Å (2 2 1) planes, 3.06 Å (0 2 3) planes and 2.88 Å (0 4 0) planes. These peaks are also recorded in the diagrams of samples C and I2, together with sharp intense peaks due to anatase (1 0 1) planes at 3.52 Å and rutile (1 0 0) planes at 3.26 Å, but are absent on the diagram of

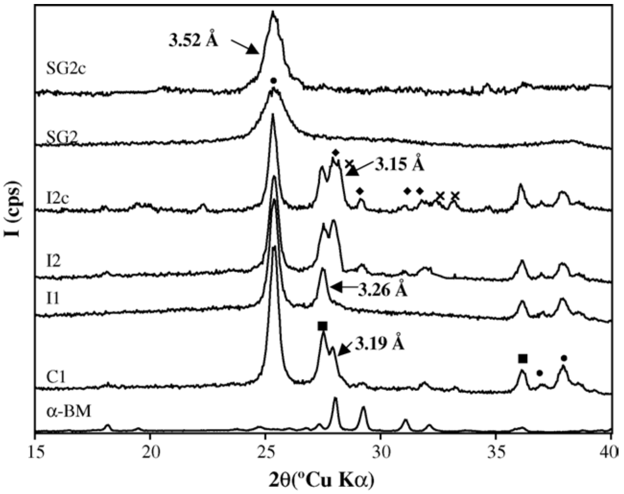

Fig. 1. X-ray diffraction patterns of Bi-Mo-Ti-O samples prepared by coprecipitation (C1), impregnation (I) and sol–gel (SG) methods. (◆) α-$Bi_2Mo_3O_{12}$, (✖) γ-Bi_2MoO_6, (●) anatase and (■) rutile.

Table 1
Crystallite sizes and specific surface areas of BM and Bi-Mo-Ti-O samples

Catalyst	D crystallite size (nm)[a]			S_{BET} ($m^2 g^{-1}$)
	α-BM	Anatase	Rutile	
α-BM	16	–	–	2
C1	22	19	16	40
I1	–	19	18	39
I2	24	19	14	27
I2c	25	43	61	29
SG2	–	12	–	108
SG2c	–	18	–	29

[a] Average crystallite size determined by X-ray diffraction line broadening.

sample I1, indicating a better dispersion of the supported phase. Prolonging the calcination time (sample I2c) favours partial transformation from α-$Bi_2Mo_3O_{12}$ to γ-Bi_2MoO_6 (koechlinite, peak most intense at 3.15Å (1 3 1) planes). Only broad peaks, i.e., broader than for the other samples, due to anatase are recorded in the diagram of samples SG2 and SG2c. Diffraction maxima due to α-BM were not observed for any of both samples, despite the different calcination time (30 min or 20.5 h) both samples have been submitted to.

The estimated cystallite sizes (D) of phase α-BM were close to 23 nm for samples C1, I2 and I2c (Table 1). The crystallite size of the titania particles also depends on the preparation method, being close to 16–19 nm for samples prepared by impregnation and coprecipitation, and to 12 nm for samples prepared via the sol–gel route. The size of the titania crystallites is appreciably enlarged as the calcination time is increased for samples I2c and SG2c, but the same crystallite sizes were determined for the α-BM phase in samples I2 and I2c.

The FT-Raman spectrum of sample α-BM shows (Fig. 2) bands at 957, 926, 902, 859, 842, 818, 669 and 652 cm^{-1}, due to stretching modes of three crystallographically unequivalent units in α-$Bi_2Mo_3O_{12}$ [9,10]. Weak bands due to this phase, together with stronger bands of rutile (447 cm^{-1}) and anatase (645, 525 and 400 cm^{-1}) [11] are recorded for catalyst C1. However, only bands due to anatase and rutile were recorded for sample I1, with the same BM loading as sample C1, and characteristic bands of α-BM and of MoO_3 (820 and 990 cm^{-1}) are only recorded when the BM loading is increased (sample I2). The enhanced intensity of the band at 820 cm^{-1} with respect to that at 902 cm^{-1} (the most intense band due to α-BM) in sample I2c is due to overlapping of modes due to MoO_3 and α-BM. The presence of bands due to α-$Bi_2Mo_3O_{12}$, γ-Bi_2MoO_6 (793 cm^{-1}) and bulk MoO_3 in the spectrum of sample I2c further confirms the α → γ partial transformation concluded from the PXRD studies [12]. However, in agreement with the PXRD data, only lines due to anatase are recorded in the spectra of samples SG2 and SG2c, together with a broad unstructured band between 700 and 950 cm^{-1} which might be tentatively ascribed to amorphous bismuth molybdate.

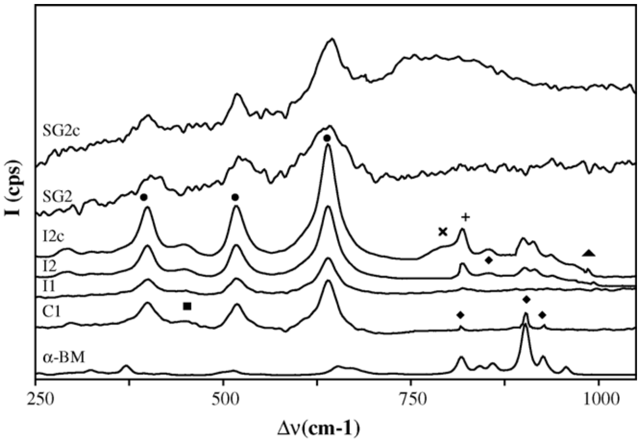

Fig. 2. FT-Raman spectra of Bi-Mo-Ti-O samples prepared by coprecipitation (C1), impregnation (I) and sol–gel (SG) methods. (◆) α-$Bi_2Mo_3O_{12}$, (✖) γ-Bi_2MoO_6, (●) anatase, (■) rutile, (▲) MoO_3 and (+) MoO_3 and α-$Bi_2Mo_3O_{12}$.

The nitrogen adsorption–desorption isotherms for all catalysts correspond to mesoporous samples; most correspond to type II in the IUPAC classification [13] with a H3 type hysteresis loop, due to aggregated particles with slit-like pores, except for sample SG2, which exhibits a type IV isotherm with type H2 hysteresis loop (characteristic of solids consisting of particles crossed by nearly cylindrical channels or made by aggregates or agglomerates of spheroidal particles). The values of the BET specific surface areas [13,14] are summarized in Table 1; they mostly range from 30 to 40 $m^2 g^{-1}$, except sample SG2, for which a value of 108 $m^2 g^{-1}$ is measured. Despite the appreciable decrease in the specific surface area upon increasing the calcination time for sample SG2 (73%), the bismuth molybdate phases still remain dispersed.

3.2. Reactivity

Results of the catalytic activity studies are summarized in Table 2. The last three columns in this table include acrolein yield per unit mass of catalyst, per unit mass of active phase and per surface area unit of catalyst, respectively. Titania was inactive at the temperatures tested.

Both at 400 and 420 °C, the presence of TiO_2 as the major component (75–86%) in Bi-Mo-Ti-O samples enhances the acrolein selectivity by a factor from 1.2 to 2.6 for C and I samples and by 1.4 to 2.4 for SG2c sample. The yield is also increased. In addition to the beneficial role of titania, the differences in yield and selectivity to acrolein measured for the samples tested can be explained on the basis of the different structures found for the active α-BM phase.

The lower selectivity shown by sample I1 with respect to sample C1 (despite both contain the same loading of BM and almost coincident specific surface areas) can be related to the crystallinity of the active phase in sample C1, as concluded from the PXRD and FT-Raman results above discussed. Oxide ions mobility from one site to another is much easier in the crystalline phase, through channels existing in well-formed structures, than in the amorphous phases. The results are similar to those previously reported by Han Han et al. [15] when studying bismuth molybdate catalysts supported on silica and prepared by coprecipitation or impregnation; these authors have claimed such an effect as a result of enhanced mobility of oxide ions in the lattice of metal oxide catalysts.

Table 2
Catalytic activity results of Bi-Mo-Ti-O and bulk bismuth molydate in propene oxidation to acrolein

Sample	C C_3H_6 (%)		Y C_3H_4O (%)		S C_3H_4O (%)		Y (μmol g^{-1} s^{-1})[a]		Y (μmol g^{-1} s^{-1})[b]		Y (μmol m^{-2} s^{-1})	
	400 °C	420 °C	400 °C	420 °C	400 °C	420 °C	400 °C	420 °C	400 °C	420 °C	400 °C	420 °C
α-BM	4.2	7.7	1.4	1.8	33.3	23.4	0.6	0.7	0.6	0.7	0.300	0.350
C1	13.1	17.2	7.1	9.4	54.0	54.6	2.9	3.8	20.5	27.2	0.072	0.095
I1	16.7	23.8	6.5	9.1	38.9	38.2	2.7	3.7	18.8	26.3	0.069	0.095
I2	17.5	18.9	9.3	11.4	54.7	60.3	3.8	4.7	15.2	18.7	0.141	0.174
I2c	18.0	23.0	7.6	10.4	42.2	45.2	3.1	4.3	12.5	17.1	0.107	0.148
SG2	21.8	27.8	4.0	5.5	18.3	19.8	1.6	2.3	6.6	9.0	0.015	0.021
SG2c	29.3	31.7	13.2	17.9	45.0	56.5	5.4	7.3	21.6	29.4	0.186	0.252

C, propene conversion; Y, yield in acrolein; S, selectivity to acrolein.

[a] Normalized yield per unit mass (g) of catalysts.

[b] Normalized yield per unit mass (g) of active phase.

The differences in selectivity observed for catalysts I2 and I2c can be probably related to the presence of γ-Bi_2MoO_6 (not detected in I2), together with α-$Bi_2Mo_3O_{12}$. Phases α and β contain a larger concentration of dioxomolybdenum units linked to Bi-O units than phase γ; consequently, as these groups are responsible for chemisorption of π-allyl radicals [16], the sample containing phase γ should exhibit a lower activity than the other samples for acrolein production. Moreover, a threshold crystallite size (ca. 23 nm) of the α-BM phase seems to be necessary to increase selectivity to acrolein formation.

The lower selectivity observed for sample SG2 should be undoubtedly related to the large dispersion of the bismuth molybdate phase. On increasing the calcination time (from sample SG2 to sample SG2c) a ca. 50% increase in the crystallite size of the anatase particles is observed and crystalline BM phases are still undetectable. Probably, the 2.8 times increase in selectivity to acrolein on passing from sample SG2 to sample SG2c is due to the sintering of the titania particles, which gives rise to a sharp decrease in the specific surface area (see Table 1); the size of the BM particles should also increase, but probably without reaching the size permitting detection by PXRD.

The beneficial effect of titania on the performance of these catalysts is also evidenced if normalized yields to acrolein over catalysts Bi-Mo-Ti-O and bulk α-BM are compared. An increase between 4 and 7 in normalized (per unit mass of catalyst) yield is observed for catalysts C and I, while such an increase is between 3 and 10 for catalysts SG. Moreover, if such a comparison is made for normalized (per unit mass of active phase) yield, an increase by a factor from 21 to 39 for samples C and I and by a factor from 11 to 42 for samples SG is observed.

Because of the so different specific surface areas displayed by these catalysts, an additional comparison can be made considering the normalized yield, referred to unit surface area of catalysts. Maximum yields are again calculated for catalysts I2 (where BM crystallites have been detected) and SG2c (formed by small Bi-Mo-O aggregates); however, no significant difference is observed between catalysts C1 (crystalline BM) and I1 (amorphous BM).

Activation energies also differ from one catalyst to another. The lowest values have been calculated for catalysts I2 and SG2c (12.5 kJ mol^{-1}), while larger values are obtained for catalysts I2c and SG2 (39.7 kJ mol^{-1}), maximum values being reached for catalysts C1 (41.8 kJ mol^{-1}) and I1 (58.5 kJ mol^{-1}).

4. Conclusions

A positive role of titania improving the catalytic performance of Bi-Mo-Ti-O samples prepared by different methods (namely coprecipitation, impregnation and sol–gel) with respect to bulk bismuth molybdate, has been found. Such an enhanced catalytic activity requires α-BM with a crystallite size close to 23 nm in the samples prepared by coprecipitation and impregnation. However, a lower catalytic activity is observed if smaller α-BM crystallites exist (sample SG2), but it is recovered after further calcination of the sample for 20 h (sample SG2c), due to stabilization of small Bi-Mo-O aggregates on the titania surface. In this way, supporting (methods C and I) or inserting (method SG) bismuth molybdate in a titania matrix constitutes a tool for fine tuning the crystal size of the bismuth molybdate, finding that crystallites should not be too small nor too large, and the optimum size of 23 nm has been found for improving the catalytic performance in partial oxidation of propene to acrolein.

The differences observed in the activation energy when the reaction is carried out on the different catalysts would probably arise from changes in the reaction mechanism due to the precise structure of the BM active phase.

Acknowledgment

This work was carried out within EU funded CONCORDE concerted action.

References

[1] R.K. Graselli, J.D. Burrington, J.F. Brazdil, J. Chem. Soc. Faraday Disc. 72 (1982) 203.

[2] D. Carson, G. Coudurier, M. Forissier, J.C. Vedrine, J. Chem. Soc. Faraday Trans. I 79 (1983) 1921.

[3] L.C. Glaeser, J.F. Brazdil, M.A. Hazle, M. Mehicic, R.K. Graselli, J. Chem. Soc. Faraday Trans. I 81 (1985) 2903.

[4] R.K. Graselli, in: G. Ertl, H. Knözinger, J. Weitkamp (Eds.), Handbook of Heterogeneous Catalysis, vol. 5, Wiley, New York, 1997, p. 2302.
[5] R.K. Graselli, Topics Catal. 21 (2002) 79.
[6] B.R. Sant, S.B. Rao, J.R. Rao, R.S. Thakur, K.M. Parida, J. Sci. Ind. Res. 43 (1984) 524.
[7] M.D. Wilberger, J.D. Grunwaldt, M. Maciejewski, T. Mallat, A. Baiker, Appl. Catal. A: Gen. 175 (1998) 11.
[8] P.A. Bastist, J.F.H. Bouwens, G.C.A. Schuit, J. Catal. 25 (1972) 1.
[9] A.F. Van Den Elzen, G.D. Rieck, Acta Crystallgr. B29 (1973) 2433.
[10] F.D. Hardcastle, I.E. Wachs, J. Phys. Chem. 95 (1991) 10763.
[11] S. Music, M. Gotié, M. Ivanda, S. Popovié, A. Turkovié, R. Trojko, A. Sekulié, K. Furié, Mater. Sci. Eng. 33 (1997) 40.
[12] S.R.G. Carrazán, C. Martín, V. Rives, R. Vidal, Appl. Catal. A: Gen. 135 (1996) 95.
[13] K.F.W. Sing, D.H. Everett, R.A.W. Haul, L. Moscou, R.A. Pierotti, J. Rouquerol, T. Siemieniewska, Pure Appl. Chem. 57 (1985) 603.
[14] S. Brunauer, P.H. Emmett, E. Teller, J. Am. Chem. Soc. 60 (1938) 309.
[15] Y. Han Han, W. Ueda, Y. Moro-Oka, Appl. Catal. A: Gen. 176 (1999) 11.
[16] J.D. Burrington, R.K. Kartisk, R.K. Grasselli, J. Catal. 81 (1983) 489.